

Mouse Mutant “Rib-Vertebrae” (*rv*): A Defect in Somite Polarity

S. NACKE,¹ R. SCHÄFER,¹ M. HRABÉ DE ANGELIS,² AND S. MUNDLOS^{1*}

¹Universitätskinderklinik Mainz, Mainz, Germany

²GSF, Institute of Experimental Genetics, Neuherberg, Germany

ABSTRACT The recessive mouse mutant rib-vertebrae (*rv*) affects the morphogenesis of the axial skeleton. The phenotype is characterized by vertebral defects such as fusion of adjacent segments, hemivertebrae, or open neural arches and rib defects including fusions, forked ribs, and additional ribs. We have analyzed this mutant in detail and are able to show that defective somite patterning underlies the vertebral malformations. The *rv* mutation leads to an elongation of the presomitic mesoderm and a disruption of the anterior-posterior polarization of somites, as indicated by the abnormal expression of *Pax1* and *Mox1*. Somites are irregular in size but the overall formation of somites appears unaffected. These changes are reminiscent of somite defects obtained in loss of function alleles of the Delta-Notch pathway. Expression of the Notch pathway components Delta-like-1 (*Dll1*) and lunatic fringe (*Lfng*) are altered in *rv* mutants. To investigate possible interactions of *rv* with components of the Notch pathway, we crossed *rv* into *Dll1^{lacZ}*. Double heterozygous (*rv/+; Dll1^{lacZ}/+*) mice show vertebral defects and homozygous animals with one inactive *Dll1* allele (*rv/rv; Dll1^{lacZ}/+*) exhibit a dramatic increase in phenotypic severity, indicating that *rv* and *Dll1* genetically interact. We have mapped *rv* to a region on chromosome 7 that is syntenic to human chromosomes 11p, 10q, and 11p. *rv* is phenotypically similar to human vertebral malformations syndromes and can serve as a model for these conditions. © 2000 Wiley-Liss, Inc.

Key words: rib-vertebrae; axial skeleton; somite; Notch-Delta; urogenital malformation; chromosome 7

INTRODUCTION

The axial skeleton consisting of vertebrae and ribs is characterized by a repetitive and segmented structure that is regionally specialized to form discrete functional entities. A number of genetically distinct phenotypes involving the axial skeleton have been described in mice and men. Whereas no specific molecular defect for non-syndromic vertebral malformations has been

detected in humans yet, several genes have been identified in the mouse that, when inactivated, result in malformed vertebrae and/or ribs. These mice are easily recognized by their malformed tails (“kink-tail” phenotype). The majority of genes that have been described in association with this phenotype are part of the Delta-Notch pathway, a signaling pathway that is of crucial importance for the formation of cell-cell boundaries (McGrew and Pourquié, 1998; Lendahl, 1998). The inactivation of *Dll3* in the mouse mutant pudgy, for example, results in severe segmentation defects with hemivertebrae, fusion of vertebrae, absent vertebrae (tail), and rib fusions (Kusumi et al., 1998). Similarly, in humans a mutation in the Delta-related Notch ligand Jagged1/Serrate1 leads to the Alagille syndrome, a dominantly inherited condition frequently associated with vertebral malformations (Li et al., 1997; Oda et al., 1997). Analysis of mice with knock-out mutations of different components or modulators of the Delta-Notch signaling pathway show irregular or defective somites suggesting that this pathway has a crucial role during somitogenesis (Barrantes et al., 1999).

Somites originate from the presomitic mesoderm (PSM), a continuous mass of cells generated in the primitive streak as it moves caudally. Cells of the newly-formed mesoderm mature and, at a certain distance from the streak, aggregate to form the somites. Recent findings have unraveled some of the basic mechanisms that control somitogenesis (Tajbakhsh and Spörle, 1998; McGrew and Pourquié, 1998; Gossler and Hrabe de Angelis, 1998). The formation of somites involves a molecular segmentation clock that leads to the oscillation of hairy1 expression in mesodermal cells. The hairy1 oscillator drives lunatic fringe expression, which in turn drives the decisive pattern of changes in Notch activity and Delta expression in the segmenting mesoderm (Aulehla and Johnson, 1999; Forsberg et al., 1998; Palmeirim et al., 1997). The Notch-Delta pathway is of crucial importance for the establishment of the periodic pattern as demonstrated by several knock-out mutations (Conlon et al., 1995,

Grant sponsor: Deutsche Forschungsgemeinschaft; Grant number: MU 880/3-1.

*Correspondence to: Stefan Mundlos, Universitätskinderklinik, Langenbeckstr.1, 55101 Mainz, Germany. E-mail: mundlos@kinder.klinik.uni-mainz.de

Received 23 March 2000; Accepted 2 June 2000

Evrard et al., 1998; Hrabe de Angelis et al., 1997; Kusumi et al., 1998; Saga et al., 1997; Zhang and Gridley, 1998). These studies have also shown that the physical periodicity is associated with a periodic pattern within the somite, giving each cell an anterior or a posterior identity. This compartmentalization is essential for the maintenance of somite borders and the restricted migration of neurons through the cranial halves of somites.

As the cells mature, the various regions of the somite become committed to form only certain cell types. Patterning of the somite is controlled by the interaction of ventralizing signals from the notochord/floorplate complex and dorsalizing signals from the surface ectoderm and neural tube. Upon these signals, the ventral medial cells of the somite undergo mitosis, become mesenchymal cells again, and migrate towards the notochord. This portion of the somite is called the sclerotome, and will eventually give rise to vertebral and rib chondrocytes. The signaling molecule sonic hedgehog (*Shh*) is the major signal from the notochord/floorplate that initiates and controls sclerotome formation (Borycki et al., 1998). Mice with inactivated *Shh* alleles develop no sclerotome and are hence devoid of the dorsal part of ribs and vertebrae (Chiang et al., 1996).

To further unravel the mechanisms of somite formation and differentiation, it is essential to isolate and characterize new genes and mechanisms involved in this process. This may be accomplished by the analysis of mouse mutants with phenotypes that are suggestive of a defect in somite formation/differentiation. We have investigated the mouse mutant rib-vertebrae (*rv*), originally identified as a spontaneous mutant in the Jackson Laboratories, Bar Harbor, Maine. *rv* is characterized by vertebral defects and rib fusions similar to other "kink-tail" mutants that can be traced back to somite defects on embryonic day 12 (Theiler and Varnum 1985). We have analyzed the *rv*-phenotype in detail and have performed chromosomal mapping of *rv*. Expression studies and crossing with other mouse mutants indicate that *rv* leads to a defect in the anterior-posterior polarization of somites via an interaction with the Delta-Notch pathway.

RESULTS

Phenotype

Affected *rv/rv* adults had reduced body length and tail kinks of different severity and frequency. The skeletal phenotype of *rv/+* and *rv/rv* mutants was analyzed on the C57BL/6J and the C57BL/6J/Cast/Ei background at several developmental time points by alcian blue/alizarin red staining. A total of 123 animals were analyzed from the B6/Cast cross. All 29 animals (24%) that were genotyped to be *rv/rv* showed some degree of skeletal involvement, whereas the other 94 animals had completely normal skeletons, indicating full penetrance for this recessive mutation. The skeletons prepared from 35 *rv/rv* animals on the C57BL/6J back-

ground were not different from those prepared from the B6/Cast cross. Full penetrance was only observed when skeletal preparations were analyzed because many of the minor abnormalities, such as additional ribs, did not result in a visible phenotype. Figure 1 shows some of the most characteristic changes. The formation of hemivertebrae and/or vertebral fusions was most frequent in the lower thoracic region (100%) and the upper cervical part of the spine (90%) whereas the lumbar region (15%) and the tail (20%) were less frequently involved. In addition, extra ribs, rib fusions, or forked ribs were a consistent finding (95%). For these experiments a total of 64 animals were examined at age 3 weeks. Considerable phenotypic variability was observed. Severely affected animals (approximately 10%) showed an involvement of the entire vertebral column whereas minor vertebral anomalies at the lower thoracic spine or a single additional rib represented the mild end of the phenotypic spectrum. Since this effect was observed on the inbred C57BL/6J background as well as on the B6/Cast background, this variability is likely to be due to stochastic events. No changes were found in the appendicular skeleton or the cranium.

We performed a detailed analysis of *rv/rv* embryos obtained from the B6/Cast *rv/+* x B6/Cast *rv/+* cross. This cross allowed genotyping of embryos using the marker *D7Mit67* or *D7Mit286*. In addition, embryos obtained from the original C57BL/6J background were also analyzed for apparent phenotypic changes. During developmental stages E11.5 to E12.5 approximately 50% of *rv/rv* embryos exhibited an enlarged tail tip and additional small buds arising laterally from the tail bud (Fig. 1G–I). Whereas in the majority of affected animals the buds are very small, some specimens showed larger buds that led to a forked tail. These findings were less frequent on the C57/Cast background. Histological analysis of the buds showed mesenchyme only. Notochord or neural tube do not penetrate into these branches. The PSM, however, appeared elongated and frequently accessory round structures were identified that most likely represent extra neural tubes. Similar changes were described by Theiler and Varnum (1985). Histology performed at later stages (E14.5) shows fusion of ganglia (Fig. 1J) and/or sclerotome condensations.

Further analysis of affected animals revealed a high frequency of urogenital malformations in *rv/rv* mice. On the C57BL/6J background, 60% of *rv/rv* mice ($n = 35$) (as identified by skeletal preparations) were affected. We observed a wide variety of phenotypes including unilateral aplasia or hypoplasia of the kidney, malrotated or displaced kidneys, or hydronephrosis due to obstruction of the ureter (Fig. 2; Table 1). In females, vaginal atresia or vagina duplex were frequent findings (of 9 *rv/rv* animals 2 were normal, 5 had vagina duplex, and 2 atresia of the vagina) whereas some of the males showed enlarged bladders with a thickened wall probably due to obstruction of the urethra by an enlarged/malformed prostate. Such anoma-

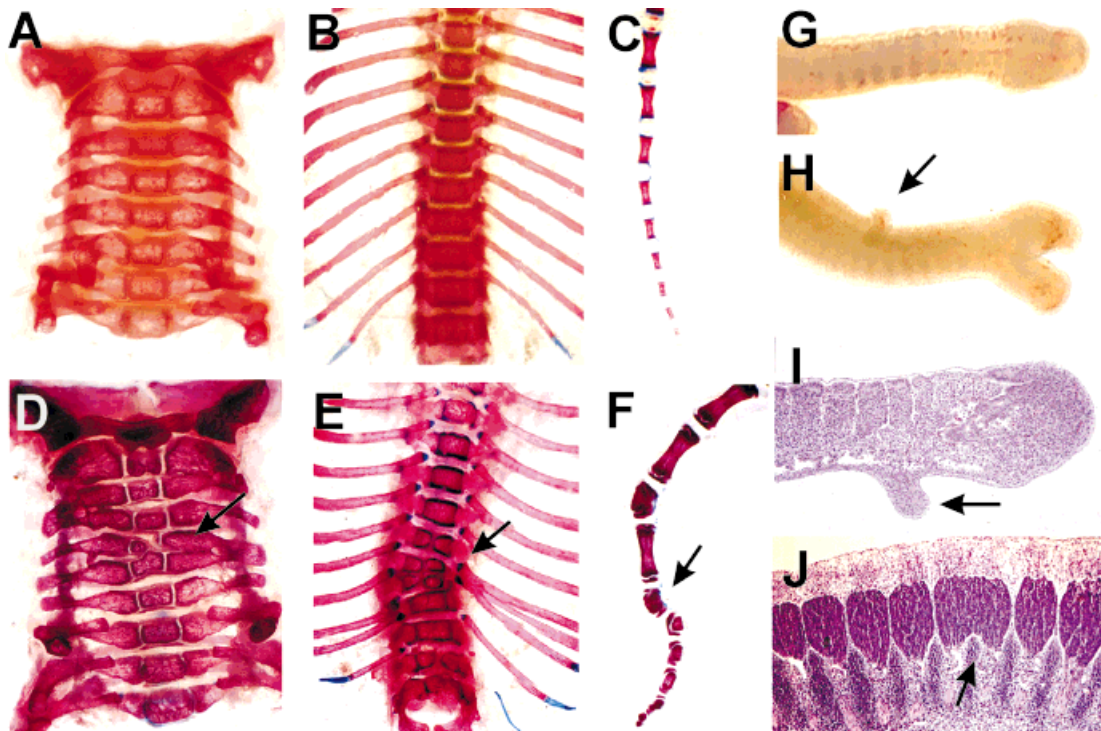


Fig. 1. The *rv/rv* phenotype. Typical skeletal changes observed in *rv/rv* mice are shown in D–F with wt skeletal preparations shown in A–C (all age 3 weeks). D: Affected cervical spine with fusion of vertebrae and hemivertebrae and (A) corresponding wt skeleton. E: Lower thoracic spine with hemivertebrae resulting in scoliosis, fusion of ribs (arrow) and additional ribs and (B) corresponding wt skeleton. F: Hemivertebrae

result in the “kink-tail” phenotype. Tail bud of wt (G) and *rv/rv* (H) embryos at stage E12.5. Note forked tail and sprouting bud (arrow) in H. I: Histological section through an *rv/rv* tail bud showing the characteristic bud that contains mesenchyme only. J: Fusion of ganglia in *rv/rv* mice, section of the lower thoracic region in a E14.5 embryo.

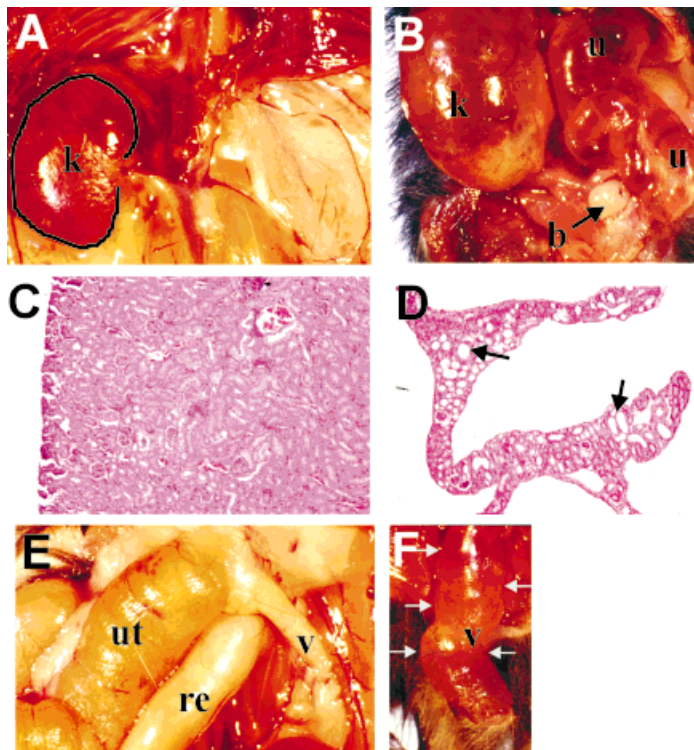


Fig. 2. Urogenital malformations in *rv/rv* mice. Urogenital malformations were a frequent feature of *rv/rv* mice when bred on the C57BL/6J background. A: Absence of left kidney, the right kidney is circled by a dotted line. B: Severely dilated ureter and hydronephrosis of the kidney in an *rv/rv* mouse. D: Section through a hydronephrotic kidney showing flattened mesenchyme with dilated collecting tubules (arrows) and (C) wt kidney (magnification $\times 50$). E: Unilateral atresia and massive dilatation of right uterine horn, and (F) vaginal atresia with dilatation of vagina (arrows) in female *rv/rv* mice. k, kidney; u, ureter; b, bladder; ut, uterus; re, rectum; v, vagina.

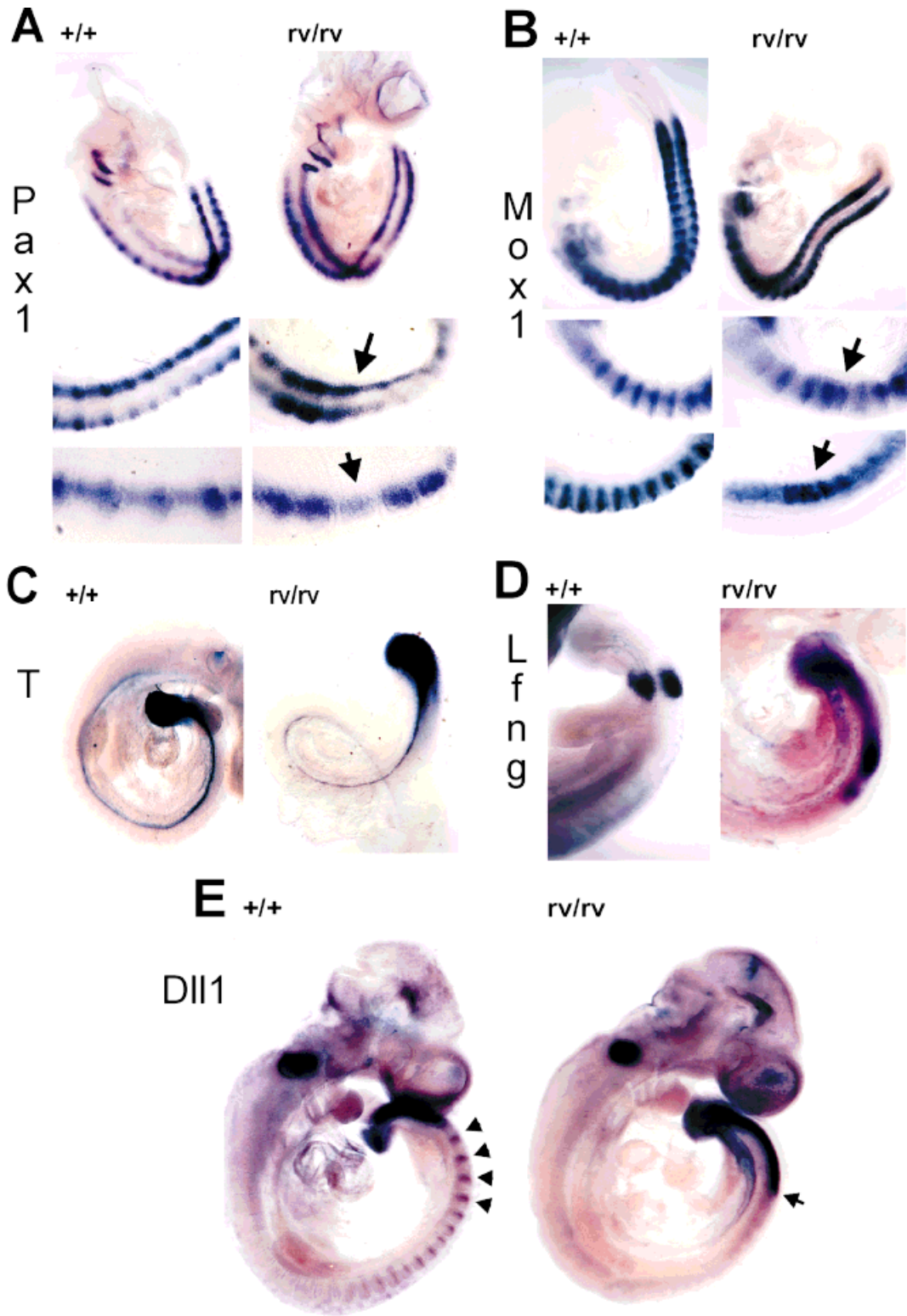


Figure 3.

TABLE 1. Malformation of the Kidney in *rv/rv* Mice

Total	Strain	Agenesis	Hydronephrosis	Cysts	Unaffected
35	C57BL/6J	15	5	1	14
55	C57BL/6J/Cast				55

lies in the males were usually not present in young mice but developed over time and were thus difficult to quantify. The breeding performance of *rv/rv* mice was poor with approximately 90% of males and females being infertile. Malformations of the kidney and/or the urogenital organs were not observed on the B6/Cast background.

Developmental Analysis

We performed whole mount in situ hybridizations with a number of probes to characterize the developmental defect in *rv/rv* mice (Fig. 3). We focused on embryos of stages E9.5 and E10.5 of development, a stage when the somites of the lower thoracic spine have already been generated, the region that is consistently affected in *rv/rv* mice.

Pax1 is expressed in the sclerotome with a stronger posterior and a weaker anterior domain. Expression of *Pax1* in the mutant was of comparable intensity to wt but the distinct domains were lost. The periodic pattern of *Pax1* expression was no longer visible and was replaced by a diffuse staining throughout the somite. The intensity of expression was variable and some somites showed strong expression whereas others showed almost absent expression of *Pax1*. Expression of *Pax1* in the branchial arches was not affected.

At E9.5 to 10.5 *Mox1* is expressed in all cell types of the somite with a stronger domain in the posterior half and a weaker domain in the anterior half. In addition, *Mox1* is expressed in the PSM that is posterior of the last somite. In the mutant, *Mox1* transcripts were strongly expressed but appeared irregular. In the tail region, *Mox1* expression was no longer defined to the posterior half of the somite, but was present throughout the entire somite. The clear segmentation characteristic for *Mox1* expression pattern was lost and replaced by a more diffuse distribution. In the more mature cranial somites, expression was again segmented but reduced and irregular with loss of expression or weak expression in single somites. Vibratome sections of these areas underlined the above findings. The integrity of the notochord was tested using probes for brachyury (*T*-gene) and *Shh* (not shown). Both were expressed in a regular pattern comparable to control litter mates. No difference was observed in the expression of *T* in the PSM.

For further analysis of the PSM, we tested the expression of lunatic fringe (*Lfng*) and Delta-1 (*Dll1*). *Lfng* is normally expressed in a wave-like pattern throughout the PSM. We found no major difference between wt and mutant embryos but the presomitic expression domain appeared expanded, less distinct, and slightly reduced. *Dll1* is expressed in the PSM and the posterior compartment of newly formed somites. In mutant embryos, expression of *Dll1* was drastically reduced or absent in the posterior part of somites. In addition, expression of *Dll1* in the PSM was expanded anteriorly in *rv/rv* embryos (Fig. 3E).

rv Interacts With the Delta-Notch Pathway

To test for interaction of *rv* with the Delta-Notch pathway, we crossed *rv* into *Dll1^{lacZ}* mice (Hrabé de Angelis et al., 1997). Double heterozygous mice (*rv/+*; *Dll1*^{+/−}) had a phenotype comparable to mild *rv/rv* with incomplete penetrance (n=12). The inactivation of one *Dll1* allele in *rv/rv* mice (*rv/rv*; *Dll1*[±]) caused additional severe vertebral malformations that were not observed in *rv/rv* or *rv/+*; *Dll1*[±] mice (n = 8). Figure 4 illustrates the most important features. Some *rv/rv*; *Dll1*[±] mice survived beyond weaning in spite of their severe skeletal malformations (n = 2). Affected mice were readily recognized by their severely shortened / absent tails. There was complete disorganization in the tail region without recognizable formation of vertebral condensations. In the rest of the spine, vertebrae were severely malformed but showed some degree of organized pattern. In the lumbar region, neighboring ver-

Fig. 3 (Overleaf). Patterning of somites in *rv/rv* embryos. **A:** Expression of *Pax1* in wt (**left**) and *rv/rv* (**right**) embryos at stage E9.5. Top: Expression pattern of *Pax1* in whole embryos. Lower two panels show vibratome sections of similar embryos (posterior is to the right). Note clearly segmented pattern in the wt embryo. The expression is strongest in the posterior part of the somite but the anterior part shows also some staining. In contrast, in *rv/rv* embryos expression is diffuse and seems not to be defined to the somite boundaries. The vibratome sections reveal expression of *Pax1* throughout the somite without clear anterior/posterior boundary. In addition, the level of expression is different between somites (arrows) with some somites having a very high expression whereas others show very low to absent expression. **B:** Expression of *Mox1* in wt (**left**) and *rv/rv* (**right**) embryos of stage E9.5. Top: Expression pattern of *Mox1* in whole embryos. Lower two panels show vibratome sections of similar embryos (posterior is to the right). Note clearly segmented pattern in the wt embryo with the expression being strongest in the posterior part. Vibratome sections of *rv/rv* embryos show an irregular expression in more cranial somites (middle panel, right side, arrow) and a diffuse staining pattern (bottom panel, right side, arrow) in the more caudal somites, when compared to controls (middle and lower panel, left side). **C:** Expression of *T* in wt (**left**) and *rv/rv* embryos (**right**). No difference in expression in the notochord or the PSM. **D:** Expression of *Lfng* in wt (**left**) and *rv/rv* (**right**) embryos. Normal expression, but elongated PSM in the *rv/rv* embryo. **E:** Expression of *Dll1* in wt (**left**) and *rv/rv* (**right**) embryos. Note strong expression in the PSM of both embryos, but lack of expression in the dorsal part of somites (indicated by arrows in wt) in the *rv/rv* embryo. The PSM appears elongated in the *rv/rv* embryo (arrow).

tebrae fused to build bony plates that covered the entire lumbar spine. This resulted in fusion of approximately half of the lumbar part of the dorsal rib cage. The cervical spine was also severely malformed. The thorax of *rv/rv*; *Dll1* \pm mice was short and broad and the insertion of ribs into the sternum was frequently asymmetric. The type and the severity of malformations made the distinction between the *rv/rv* and the *rv/rv*; *Dll1* \pm phenotypes unambiguous.

No Apparent Interaction of *rv* With the Shh Pathway

To test for a possible interaction of *rv* with the Shh pathway, the major ventral signal for somite differentiation, we crossed *rv* into *Dsh/+* mice. *Dsh* (short digit) is a radiation-induced mutant that shows in the homozygous state phenotypic overlap with the phenotype of *Shh* $-/-$ mice and that was shown to be allelic to *Shh* (Mundlos, unpublished observation). Heterozygous *Dsh* mice can easily be recognized by their fore-shortened digits. The crossing of *Dsh* into *rv/rv* revealed no additional phenotypes. *rv/rv*; *Dsh/+* animals demonstrated the typical changes described for both mutants, i.e., vertebral malformations and short digits but there were no synergistic effects.

Genetic Mapping

The crossing of *rv* on the C57BL/6J background with *M. musculus castaneus* (Cast/Ei) allowed easy mapping. For the initial genome scan DNA from 29 homozygous *rv* progeny from the F1 intercross (as judged by skeletal preparations) was used. These results suggested linkage to chromosome 7. The analysis of additional markers confirmed the results and located *rv* to chromosome 7 in a region between 61 and 63 cM. Testing of another 46 affected and 94 unaffected mice (as judged by skeletal preparations) narrowed the critical interval containing the *rv* gene to a region between the markers *D7Mit68* and *D7Mit106*, each defined by one recombination. This interval contains the markers *D7Mit67* and *D7Mit286*, which were non-recombinant in 75 affected and 94 unaffected animals. The results are summarized in Figure 5.

DISCUSSION

In the present article we describe phenotype, mapping, and developmental analysis of the rib-vertebrae (*rv*) mutation. *rv* is a recessive mutation with full penetrance in the homozygote. Homozygous animals can be recognized by their kink tails and short bodies. However, approximately half of the affected animals do not have a visible phenotype and skeletal preparations are necessary to identify more subtle changes. Typical changes include missing parts of vertebrae (hemivertebrae), fusions of neighboring vertebrae, rib fusions, and additional ribs. Similar observations were made in the original description of *rv* by Theiler and Varnum (1985). The combination of abnormalities observed in *rv* suggests a defect in somitogenesis.

Recently much progress has been made in unraveling the molecular mechanisms of somitogenesis through the generation of knock-out experiments. Whereas some genes seem to be essential for establishing the basic metameric pattern or for epithelial somite morphogenesis, others, like Notch1, Delta-like-1 (*Dll1*), Delta-like-3 (*Dll3*), *RBPJ κ* or presenilin are crucial for defining half-somite identities. The latter are part of the Notch-Delta pathway, a signaling system originally described in *Drosophila* where it controls cell-fate choice in the lateral inhibition process. In this model, transmembrane receptors of the Delta/Serrate family signal to Notch receptors on a neighboring cell, which results in the intracellular cleavage of the receptor, the transport of cleaved fragment into the nucleus its binding to an effector protein (*RBPJ κ*) and the subsequent activation of downstream genes (Lendahl, 1998). If genes of this pathway are inactivated, they exhibit a strong segmentation phenotype with uncoordinated formation of somites of variable sizes (Conlon et al., 1995; Evrard et al., 1998; Hrabé de Angelis et al., 1997; Kusumi et al., 1998; Saga et al., 1997; Zhang and Gridley, 1998). However, epithelial somites are formed in these mutants indicating that genes of the Notch pathway might not be important for cellular differentiation in the PSM but rather for coordinating somite morphogenesis. Further studies demonstrated that the expression of segmental markers was highly abnormal in these mutants indicating that the subdivision of each sclerotome in anterior and posterior compartments is profoundly altered, a process that was shown to be independent of somite formation (Barrantes et al., 1999).

Similar observations were made in *rv/rv* mutants. Whereas the overall formation of somites appeared to not to be affected by the mutation, the anterior-posterior compartmentalization of somites was clearly perturbed. The analysis of a marker for sclerotome differentiation, *Pax1*, confirmed the presence of cellular differentiation products of somites. However, in contrast to wt embryos, which show a clearly segmented pattern of *Pax1* expression, expression of mutant embryos was diffuse without the strong expression in the posterior segment half. Expression was frequently irregular and poorly defined. Another marker for somite segmentations, *Mox1* gave similar results. Normally expressed in all cell types of somites (Candia et al., 1992), exhibiting a domain of weak expression in the anterior and a domain of strong expression in the posterior of somites, *Mox1* was no longer differentially expressed in *rv/rv* embryos but gave a diffuse pattern and seemed to be present at similar levels. These results are similar to those obtained in *Dll1* mutants (Hrabé de Angelis, 1997) and other mutants of the Notch pathway.

The subdivision of somites into posterior and anterior compartments is a product of signaling in the PSM. A wave front model has been proposed where the oscillating expression of c-hairy in the PSM drives the ex-

pression of *Lfng*, which in turn interacts with Notch signaling. Studies in *Lfng*, *Dll1*, *Dll3*, *Notch1*, *RBPJ κ* , and *Mesp2* mutant mice demonstrate that the perturbation of Notch signaling leads to a general patterning disruption of the PSM (Barrantes et al., 1999). The characteristic expression of markers for both the anterior and the posterior somite halves is lost, which results in an abnormal compartmentalization of somites. For example, Heitzler et al. (1996) showed that *Dll1*, which in wt embryos is expressed in the PSM, the primitive streak and the posterior half of prospective and mature somites, is severely down-regulated in the posterior somite halves of *RBPJ κ* and *Notch1* mutant embryos. However, the expression in the PSM appeared unaffected. We found very similar alterations in *rv/rv* embryos with absent or suppressed expression in somites and normal expression in the PSM. Barrantes et al. (1999) describes only slightly reduced expression with less defined borders of *Lfng* expression in *Notch1* mutants, indicating that *Lfng* is a target of Notch signaling in the PSM. Again, we obtained very similar results in *rv/rv* embryos.

The typical skeletal phenotype, the perturbation of anterior-posterior somite boundaries with the loss of differentiated expression of marker genes, and the alterations in the expression of *Dll1* and *Lfng* suggested that *rv* might be part of the Notch signaling pathway. To test this hypothesis, we crossed *Dll1^{lacZ}* mice into *rv*-mice. The double mutant mice (*rv/rv*; *Dll1 \pm*) exhibited a strong phenotype that was clearly different and more severe than the *rv/rv* phenotype. Thus, *Dll1* and *rv* interact on a genetic basis indicating that *rv* is part of the Delta-Notch pathway.

The penetrance of urogenital malformations is dependent on the background. They point to the fact that the *rv*-gene has, in addition to its role in somitogenesis, a role during development of the male and female urogenital tract. Absence of kidneys and hydronephrosis due to obstruction of the ureter suggest a role for *rv* during outgrowth of the ureteric bud and/or during mesenchymal induction of the metanephric blastema. The combination of urogenital malformations and malformations of the axial skeleton is a frequent finding in patients with spondylocostal dysostosis, a condition that exhibits many phenotypic similarities with *rv* (Mortier et al., 1996). It is thus likely that mutations in the human *rv*-homologue will be the causative for at least some of these conditions.

Mapping of the *rv*-phenotype placed the *rv*-gene on chromosome 7 between the markers *D7Mit68* and *D7Mit106* in a region that is syntenic to human chromosomes 11p15.5–11p15.4, 10q24–10q26, and 16p13.1–13p11. So far, vertebral segmentation defects have been associated with a deletion of chromosome 18q22.2 —qter (Dowton et al., 1997), a translocation t(9;15)(q32;q21.1) (Crow et al., 1997) and chromosome 19q13.1–q13.3 (Turnpenny et al., 1999). Thus, no spondylocostal phenotype has been mapped to a region syntenic to the *rv*-

region. The present study opens new avenues for cloning of the *rv*-gene, a potential interactor of the Delta-Notch pathway and likely candidate for human conditions involving malformations of the urogenital system and the axial skeleton.

EXPERIMENTAL PROCEDURES

Mice, Chromosomal Mapping

Rib-vertebrae (*rv*) and *M. musculus castaneus* (Cast/Ei) mice were obtained from the Jackson Lab, Bar Harbor, Maine. *rv* arose in C57BL/6 and was subsequently maintained on the C57BL/6J background. Our initial analysis of the urogenital and the skeletal phenotype was performed on this background by breeding *rv/+* \times *rv/+* or *rv/rv* \times *rv/+*. For mapping purposes, C57BL/6J; *rv/rv* was crossed with Cast/Ei. Intercross animals were obtained by mating (*rv/+* \times Cast/Ei)F1 with (*rv/+* \times Cast/Ei)F1. Skeletal preparations were obtained from 123 animals for a definite phenotypic analysis. The B6/Cast cross was also used to assess the penetrance and variability of the skeletal phenotype. DNA used for genetic mapping was prepared from tail biopsy samples. Microsatellite markers (Dietrich et al., 1992) were analyzed by PCR and the products visualized on ethidium bromide stained agarose gels.

Phenotype and Developmental Analysis

Phenotypic analysis was performed on the C57BL/6J background and on the B6/Cast cross. For analysis of mutant embryos, timed matings were produced and noon of the day a vaginal plug was observed was counted as day 0.5 of gestation. For analysis of the skeletal phenotype, animals were sacrificed at age 3 weeks and skeletal preparations were done as described in Mundlos (2000). *rv/rv* mice were identified by their skeletal changes and, in the case of the B6/Cast cross, by genotyping using the markers *D7Mit67* or *D7Mit286*. These markers are polymorphic between C57BL/6J and Cast/Ei and are close to the *rv*-gene (see results section genetic mapping). Analysis and description of the *rv/rv* skeletal phenotype was based on skeletal preparations of 35 animals from the C57BL/6J cross and 29 animals (genotyped *rv/rv*) from the B6/Cast cross. A total of 65 heterozygous animals (genotyped *rv/+*) were compared to 27 wt litter mates to determine possible changes in *rv/+* animals. The kidney phenotype was analyzed in 35 *rv/rv* C57BL/6J animals (as determined by skeletal preparations) and in 55 genotyped *rv/rv* mice of the B6/Cast cross. For histological analysis, embryos and tissues from adult animals were embedded in paraffin or in methacrylate (Historesin, Leica) and sectioned at 7 or 3 μ m, respectively.

To test a possible interaction of *rv* with the Delta-Notch pathway, we crossed *rv* into *Dll1^{lacZ}* mice (Hrabé de Angelis, 1997). This was performed by crossing *rv/rv* mice from the B6/Cast cross with *Dll1^{lacZ/+}* mice to obtain *rv/+*; *Dll1^{lacZ/+}* mice. Homozygous *rv/rv* mice with one *Dll1^{lacZ}* allele were obtained by crossing *rv/+*;

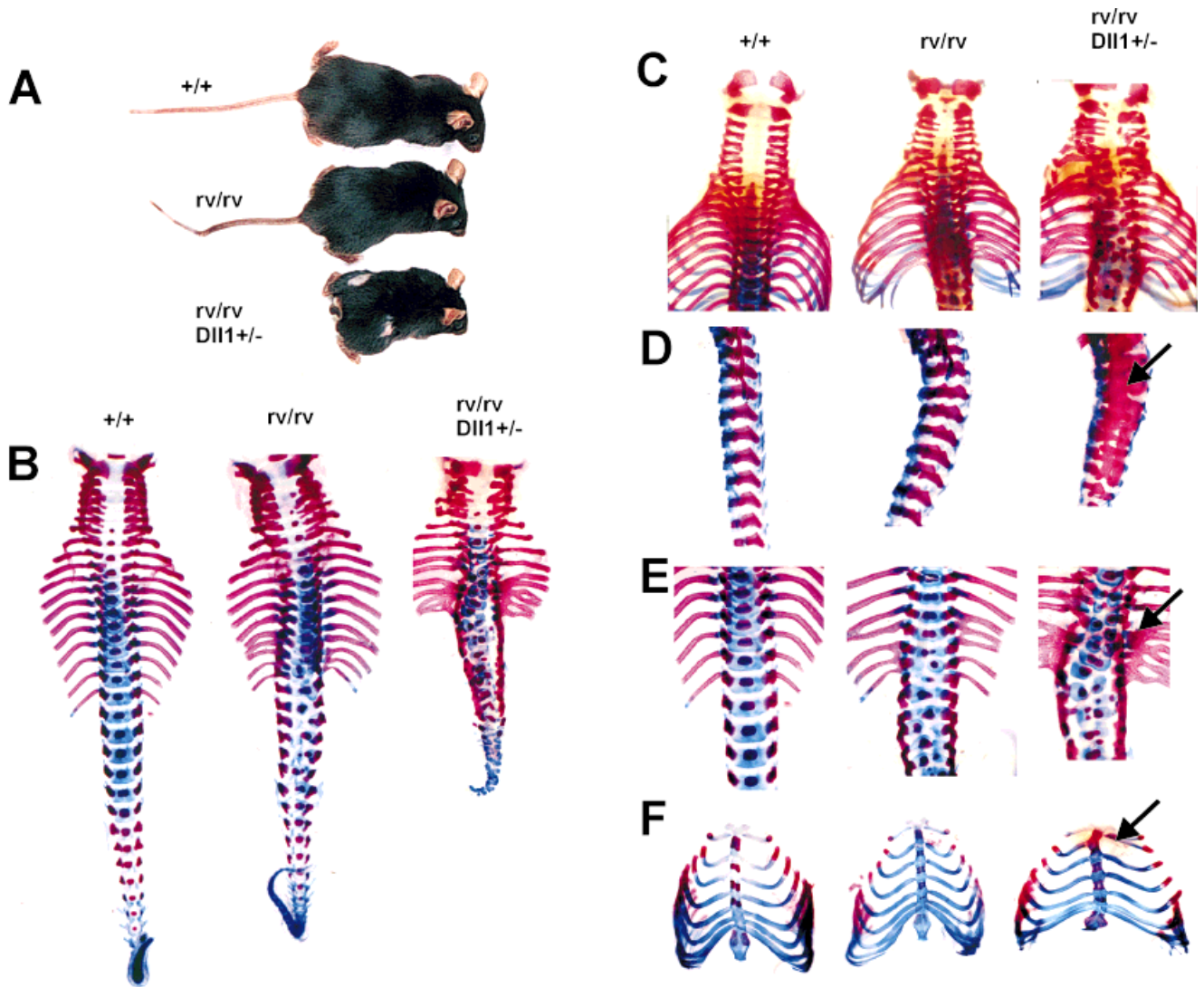


Fig. 4. The *rv/rv; Dll1±* phenotype. **A:** wt, *rv/rv*, and *rv/rv; Dll1±* mice of the same litter age 3 months. Note kink-tail in *rv/rv* and very short/absent tail in the *rv/rv; Dll1±* mouse. **A–F:** Skeletal preparations of wt, *rv/rv*, and *rv/rv; Dll1±* embryos of one litter, stage E16.5 **B:** Ventral view of entire axial skeleton. Note short tail and disorganization of vertebrae in the *Dll1±* embryo. **C:** Dorsal view of cervical and thoracic spine and ribs. **D:** Side view of lumbar vertebrae. Note almost complete fusion (arrow) of

vertebrae in the double mutant embryo. **E:** Ventral view lower thoracic/upper lumbar region. Note rib fusions and irregularities in vertebrae in the *rv/rv* skeleton. Severe rib fusion (arrow), short spine, and severe derangement of vertebrae in the *rv/rv; Dll1±* embryo. **F:** Ventral view of thorax showing absent rib (arrow) and irregular insertion of ribs in the double mutant.

Dll1^{lacZ/+} × (*rv/rv*) and (*rv/+; Dll1^{lacZ/+}*) × (*rv/+; Dll1^{lacZ/+}*) mice. A total of 6 litters (3 each) were examined at E16.5 and 2 at the age of 3 weeks. Skeletons were prepared as described in Mundlos (2000). Genotyping of *Dll1^{lacZ/+}* mice was performed as described (Hrabé de Angelis, 1997) and/or by amplifying the neomycin cassette present in this construct with the primers *tctggattcatcgactgtgg* and *gatccctcagaagaactcgt*.

Whole-mount in situ hybridization was performed as described (Henrique et al., 1995). Embryos of stage E9.5 and E10.5 were obtained by timed matings from the *rv/+; B6/Cast* cross. Genotyping was performed with DNA

from extraembryonic membranes using the markers *D7Mit67* or *D7Mit286*. The probes used for whole mount in situ hybridization were specific for *Pax1*, *Mox1*, *LFng*, *Dll1*, *T*, *Shh* (Mundlos, 2000). We tested 4–6 mutant embryos or each probe and stage and compared them with embryos from the same litter. Probes were generated by RT-PCR from mouse embryos E10.5 with the T7 promoter sequence added to the 3 primer as described in Mundlos (2000). Vibratome sections of whole-mount stained embryos were cut at 50–100 μm thickness after embedding in a mixture of gelatin/albumen/sucrose. Sections were mounted onto slides and photographed.

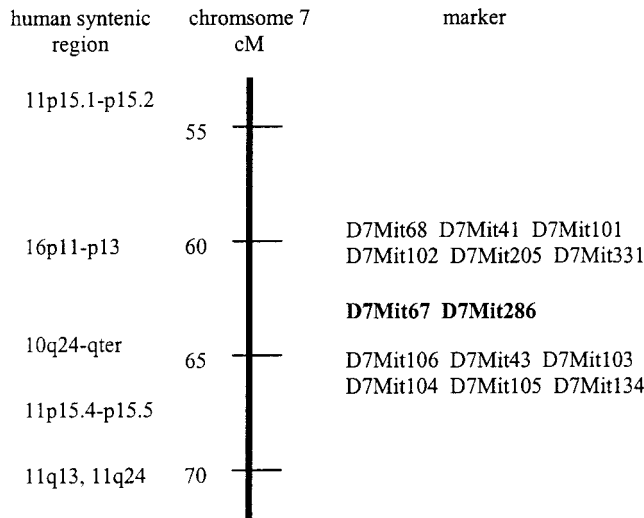


Fig. 5. Chromosomal localization of *rv*. Human syntenic regions and cM position according to <http://www.informatics.jax.org>. Non-recombinant marker are indicated in bold.

REFERENCES

- Aulehla A, Johnson RL. 1999. Dynamic expression of lunatic fringe suggests a link between notch signaling and an autonomous cellular oscillator driving somite segmentation. *Dev Biol* 207:49–61.
- Barrantes IB, Elia AJ, Wunsch K, Hrabé-deAngelis MH, Mak TW, Rossant J, Conlon RA, Gossler A, delaPompa JL. 1999. Interaction between Notch signalling and Lunatic fringe during somite boundary formation in the mouse. *Curr Biol* 9:470–480.
- Borycki AG, Mendham L, Emerson CP Jr. 1998. Control of somite patterning by Sonic hedgehog and its downstream signal response genes. *Development* 1;125:777–790.
- Candia AF, Hu J, Crosby J, Lalley PA, Noden D, Nadeau JH, Wright CV. 1992. Mox-1 and Mox-2 define a novel homeobox gene subfamily and are differentially expressed during early mesodermal patterning in mouse embryos. *Development* 116:1123–1136.
- Chiang C, Litingtung Y, Lee E, Young KE, Corden JL, Westphal H, Beachy PA. 1996. Cyclopia and defective axial patterning in mice lacking Sonic hedgehog gene function. *Nature* 383:407–413.
- Conlon RA, Reaume AG, Rossant J. 1995. Notch1 is required for the coordinate segmentation of somites. *Development* 121:1533–1545.
- Crow YJ, Tolmie JL, Rippard K, Nairn L, Wilkinson AG, Turner T. 1997. Spondylocostal dysostosis associated with a 46, XX, +15, dic(6;15)(q25;q11.2) translocation. *Clin Dysmorphol* 6:347–350.
- Dietrich WF, Miller JC, Steen RG, Merchant M, Damron D, Nahf R, Gross A, Joyce DC, Wessel M, Dredge RD, et al. 1997. A genetic map of the mouse with 4,006 simple sequence length polymorphisms. *Nat Genet* 7:220–245.
- Downton SB, Hing AV, Sheen-Kaniecki V, Watson MS. 1997. Chromosome 18q22.2—qter deletion and a congenital anomaly syndrome with multiple vertebral segmentation defects. *J Med Genet* 34:414–417.
- Evrard YA, Lun Y, Aulehla A, Gan L, Johnson RL. 1998. Lunatic fringe is an essential mediator of somite segmentation and patterning. *Nature* 394:377–381.
- Forsberg H, Crozet F, Brown NA. 1998. Waves of mouse Lunatic fringe expression, in four-hour cycles at two-hour intervals, precede somite boundary formation. *Curr Biol* 8:1027–1030.
- Gossler A, Hrabé de Angelis M. 1998. Somitogenesis. *Curr Top Dev Biol* 38:225–287.
- Heitzler P, Bourouis M, Ruel L, Carteret C, Simpson P. 1996. Genes of the Enhancer of split and achaete-scute complexes are required for a regulatory loop between Notch and Delta during lateral signalling in *Drosophila*. *Development* 122:161–171.
- Henrique D, Adam J, Myat A, Chitnis A, Lewis J, Ish-Horowitz D. 1995. Expression of a Delta homologue in prospective neurons in the chick *Nature* 375:787–790.
- Hrabé de Angelis M, McIntyre J 2nd, Gossler A. 1997. Maintenance of somite borders in mice requires the Delta homologue Dll1. *Nature* 386:717–721.
- Kusumi K, Sun ES, Kerrebrock AW, Bronson RT, Chi DC, Bulotsky MS, Spencer JB, Birren BW, Frankel WN, Lander ES. 1998. The mouse pudgy mutation disrupts Delta homologue Dll3 and initiation of early somite boundaries. *Nat Genet* 19:274–278.
- Lendahl U. 1998. A growing family of Notch ligands. *Bioessays* 20:103–107.
- Li L, Krantz ID, Deng Y, Genin A, Banta AB, Collins CC, Qi M, Trask BJ, Kuo WL, Cochran J, Costa T, Pierpont ME, Rand EB, Piccoli DA, Hood L, Spinner NB. 1997. Alagille syndrome is caused by mutations in human *Jagged1*, which encodes a ligand for Notch1. *Nat Genet* 16:243–251.
- McGrew MJ, Pourquie O. 1998. Somitogenesis: segmenting a vertebrate. *Curr Opin Genet Dev* 8:487–493.
- Mortier GR, Lachman RS, Bocian M, Rimoin DL. 1996. Multiple vertebral segmentation defects: analysis of 26 new patients and review of the literature. *Am J Med Genet* 61:310–319.
- Mundlos S. 2000. Skeletal morphogenesis. In: Tuan RS, Lo CW, editors. *Methods in molecular biology*, Vol. 136: developmental biology protocols, Vol. II. Totowa, NJ: Humana Press Inc. p 61–75.
- Oda T, Elkahoun AG, Pike BL, Okajima K, Krantz ID, Genin A, Piccoli DA, Meltzer PS, Spinner NB, Collins FS, Chandrasekharappa SC. 1997. Mutations in the human *Jagged1* gene are responsible for Alagille syndrome. *Nat Genet* 16:235–242.
- Palmeirim I, Henrique D, Ish Horowitz D, Pourquie O. 1997. Avian hairy gene expression identifies a molecular clock linked to vertebrate segmentation and somitogenesis. *Cell* 91:639–648.
- Saga Y, Hata N, Koseki H, Taketo MM. 1997. *Mesp2*: a novel mouse gene expressed in the presegmented mesoderm and essential for segmentation initiation. *Genes Dev* 11:1827–1839.
- Tajbakhsh S, Spörle R. 1998. Somite development: constructing the vertebrate body. *Cell* 92:9–16.
- Theiler K, Varnum DS. 1985. Development of rib-vertebrae: a new mutation in the house mouse with accessory caudal duplications. *Anat Embryol Berl* 173:111–116.
- Turnpenny PD, Bulman MP, Frayling TM, Abu Nasra TK, Garrett C, Hattersley AT, Ellard S. 1999. A gene for autosomal recessive spondylocostal dysostosis maps to 19q13.1-q13.3. *Am J Hum Genet* 65:175–182.
- Zhang N, Gridley T. 1998. Defects in somite formation in lunatic fringe-deficient mice. *Nature* 394:374–377.